XVI International Conference on Computational Plasticity. Fundamentals and Applications
COMPLAS 2021
E. Oñate, D. Peric, M. Chiumenti and Eduardo de Souza Neto (Eds)

INFLUENCE OF RATE DEPENDENT PLASTICITY ON A SHEET METAL BENDING PROCESS

Christian Reisinger[§*], Christian Zehetner[§], Hans Irschik[†], Michael Krommer[†] and Wolfgang Kunze[Y]

[§] University of Applied Sciences Upper Austria
Stelzhammerstraße 23, 4600 Wels, Austria
e-mail: christian.reisinger@fh-wels.at, web page: http://www.fh-ooe.at/

[†] Institute of Technical Mechanics, Johannes Kepler University Linz
Altenbergerstraße 69, 4040 Linz, Austria
e-mail: michael.krommer@jku.at - Web page: http://www.jku.at/tmech

[Y] Salvagnini Maschinenbau GmbH
Dr.-Guido-Salvagnini-Straße 1, 4482 Ennsdorf, Austria
e-mail:wolfgang.kunze@salvagninigroup.com - Web page: http://www.salvagnini.at

Key words: Plasticity, rate dependent plasticity, beam theory, extended Hollomon

Abstract. The high demands on precision and quality of industrial sheet metal forming processes are increasing steadily. Therefore, more and more effects concerning the machines but also the material behaviour of the workpiece must be considered. Here, we consider an automatic panel bender of Salvagnini Maschinenbau GmbH [1]. In this application, it turned out that the speed of bending is a relevant influence factor.

Goal of this work is to estimate the influence of strain rate on bending forces and the shape of the bent profile. In a previous work [2], an analytic model in the framework of Bernoulli-Euler beam theory for the bending of a cantilever with elasto-plastic behaviour has been presented, dimensionless influence parameters have been derived, and it has been shown that the influence parameters obtained by linear beam theory are also relevant for the nonlinear industrial application involving large deformations. To include the strain rate dependency, the beam model now has been extended to elasto-visco-plastic behaviour. Besides the plastic deformations also the elastic ones are important, since the springback angle must be known exactly to achieve the required accuracy. To represent this effect, Hollomon's equation [3] was extended by an elastic term. Additionally, the strain rate sensitivity is considered according to [9].

With this beam model, numerical studies have been performed, in which forces, and deflections have been analysed for small deformations. Finally, the results of beam theory have been compared with 3D-Finite Element computations. A very good coincidence turned out. The results also show that the strain rate has a significant influence on deformations and forces. The outcome of the present study will be used to consider the strain rate as an additional parameter in the digital twin of the automatic panel bender [1].

1 INTRODUCTION

The high demands on the metal forming industry are steadily increasing. On the one hand, the demand on precision is increasing, and on the other hand, production time has to be reduced. For this purpose, more and more effects concerning the machine, but also the material behavior of the workpiece must be taken into account. Here, we consider an automatic panel bender from Salvagnini Maschinenbau GmbH [1] which enables the fabrication of complete products from plane metal sheets. In this application it was shown that an exact modelling of the material is necessary, and that the speed of the bending process is an important influence factor.

In the literature, there are a lot of models for the description of the material behavior, e.g. the models of Hollomon [3], Ludwik [4] or Voce [5] are well known and frequently applied. All these material models describe the quasi-static flow, i.e they are obtained by tensile tests with a very low speed. In a previous paper [2], the plastic behaviour of the material was analysed in detail using a cantilever beam, representing the material behaviour by the Hollomon equation

$$\sigma(\varepsilon) = a\ \varepsilon^n, \tag{1}$$

which describes the relation between the Cauchy stress σ and the Hencky strain ε in exponential form. In Eq. (1), a is the strength coefficient, and n the hardening exponent, both to be determined by quasi-static tensile tests.

In this work, we additionally want to take into account the influence of the bending speed on the final shape of the workpiece. Therefore, the influence of the strain rate $\dot{\varepsilon} = \frac{d}{dt}\varepsilon$ must be considered in the material model. Several variants of rate-dependent material laws can be found in the literature. Many of them are extensions of the quasi-static models, e. g. the extended Hollomon equation [6], the model of Johnson Cook [7], or also the model of Cowper Symonds [8].

For the selection of the appropriate material law, there are several aspects: First, this study is performed in the framework of Bernoulli Euler beam theory according to [2]. Secondly, the strain rates are moderate in the considered industrial bending process. Considering both aspects, the model presented in [9] is used, extending the quasi-static flow curve by a multiplicative rate-dependent term as

$$\sigma(\varepsilon, \dot{\varepsilon}) = \sigma(\varepsilon, \dot{\varepsilon}_0) \left(\frac{\dot{\varepsilon}}{\dot{\varepsilon}_0} \right)^m, \tag{2}$$

where m is the strain rate sensitivity, and $\dot{\varepsilon}_0$ is the reference strain rate underlying in the quasi-static flow curve, Eq. (1). In Eq. (2) the Cauchy stress $\sigma = \sigma(\varepsilon, \dot{\varepsilon})$ now is a function of strain ε and the strain rate $\dot{\varepsilon}$. Here, $\dot{\varepsilon} \leq \dot{\varepsilon}_0$ is the quasi-static case, ie. the strain rate is lower than the reference strain rate, such that $\sigma(\varepsilon) = \sigma(\varepsilon, \dot{\varepsilon}_0)$. According to [9], Eq. (2) holds for strain rates up to $1s^{-1}$ which is sufficient for the considered material and process. Compared to more complicated material laws in the literature, the chosen model is also beneficial for application in beam theory.

The aim of this work now is to estimate the influence of the strain rate on the bending force and geometry of the bent sheet. For this purpose, a cantilever beam with rate

dependent material behaviour according to Eq. (2) is considered in section 2. Using Bernoulli Euler beam theory, a formal relationship between the load and the curvature of the beam is derived. In section 3, the influence of the strain rate on curvature, bending angle and deflection is discussed based on the beam theory results. A comparison with the purely elastic and quasi-static elasto-plastic case is also included. Finally, in section 3.2, the theoretical results are verified by Finite Element (FE) computations in Abaqus: The agreement between beam theory and FE model is analysed in detail for a specific case. Subsequently, a parameter study is carried out, showing the parameter range for application of the proposed beam theory.

2 STRAIN-RATE-DEPENDENT BENDING OF A CANTILEVER BEAM

In the following, we consider a cantilever beam with length L, Figure 1. The cross section of the beam is rectangular with the width B and height H. The left end of the beam is clamped, and on the right side a time dependent force $P(t)$ is acting. This force causes the bending moment

$$M\left(x,t\right) = -P\left(t\right)\left(L-x\right). \tag{3}$$

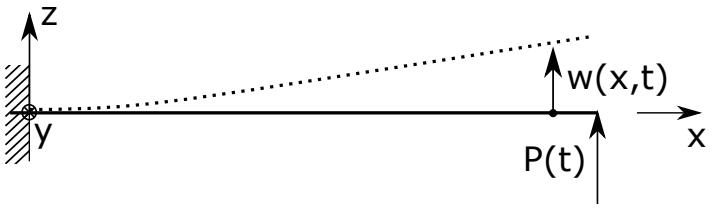

Figure 1: cantilever beam

In [2] an elasto-plastic material behavior according to Eq. (1) was analysed. In the following an extension for the strain rate dependency according to Eq. (2) is considered, in order to take into account the speed of load application, $P(t)$. For strains lower than the yield stress σ_Y, we obtain the linear elastic case according to Hooke's Law, $\sigma = E\varepsilon$, with the Young modulus E. Since the strain rate in general is a function of location and time, $\dot{\varepsilon} = \dot{\varepsilon}(x,z,t)$ and the yield stress depends on the strain rate, we obtain $\sigma_y = \sigma_y(x,z,t)$. For the uni-axial state of stress (tensile test) we write

$$\sigma = \begin{cases} -a\varepsilon^n \left(\frac{\dot{\varepsilon}}{\dot{\varepsilon}_0}\right)^m, & \varepsilon \leq -\frac{\sigma_Y}{E} \\ E\varepsilon, & -\frac{\sigma_Y}{E} \leq \varepsilon \leq \frac{\sigma_Y}{E} \\ a\varepsilon^n \left(\frac{\dot{\varepsilon}}{\dot{\varepsilon}_0}\right)^m, & \varepsilon \geq \frac{\sigma_Y}{E} \end{cases}. \tag{4}$$

Note that at yield, $\sigma = \sigma_Y$, $\varepsilon = \varepsilon_Y$ the flow curve must be continuous. Thus, yield stress and strain are derived from Eq. (4) by equating line 2 (linear elastic section, Hooke)

and line 3 (plastic section). Solving the obtained equation yields

$$\sigma_Y(x,z,t) = E\varepsilon_Y, \qquad \text{with} \qquad \varepsilon_Y = \left(\frac{a}{E}\left(\frac{\dot{\varepsilon}(x,z,t)}{\dot{\varepsilon}_0}\right)^m\right)^{\frac{1}{1-n}} \tag{5}$$

Figure 2 shows the flow curves resulting from Eq. (2) for different strain rates. We can observe an additional hardening with increasing strain rate. At small strains, Figure 3, the change in yield stress can also be seen. For these figures, the identical material parameters a, n, m, $\dot{\varepsilon}_0$ and E were used as in the numerical studies in section 3.

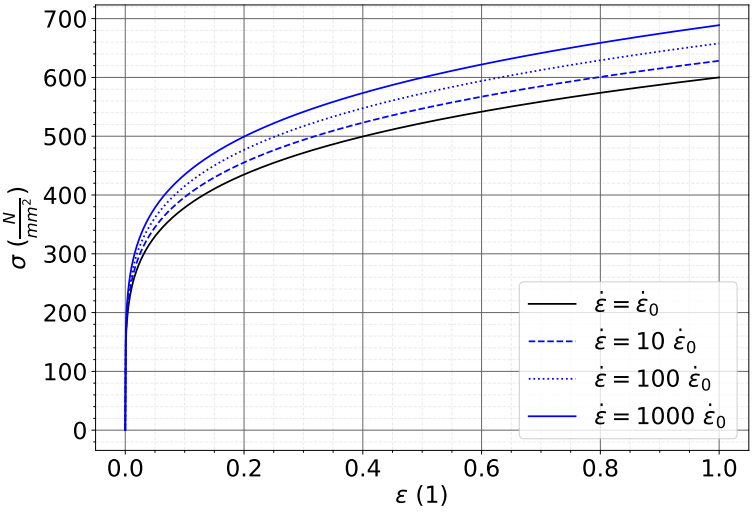

Figure 2: Theoretical dynamic flow curve model

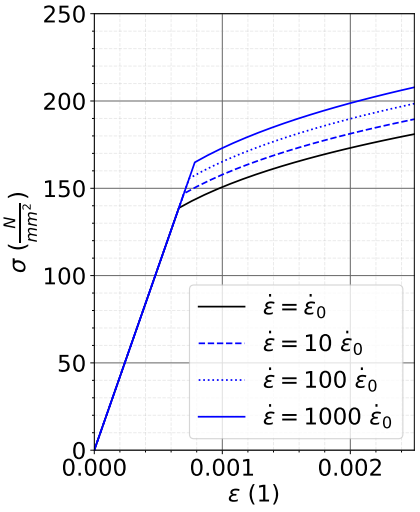

Figure 3: Theoretical dynamic flow curve model, detail

2.1 Bernoulli Euler Beam Theory

According to beam theory [10] and [11], the internal bending moment is a resultant of the stress,

$$M(x,t) = B\int_{-H/2}^{H/2} \sigma(x,z,t) z dz. \tag{6}$$

For evaluation of this integral, symmetry is utilized, and the integral is divided into two zones, a linear elastic one for $z \leq z_Y,\ \sigma \leq \sigma_Y$, and a plastic zone for $z > z_Y,\ \sigma > \sigma_Y$, where z_Y is denoted as yield height. Figure 4 schematically shows these zones. The boundary of the plastic zone is specified by the yield height $z_Y = z_Y(x,t)$, and the yield length x_Y. Note, that for $x > x_Y$ only an elastic zone exists.

Inserting Eq. (4) into (6) and considering that $\varepsilon = \varepsilon(x,z,t), \dot{\varepsilon} = \dot{\varepsilon}(x,z,t)$, we obtain

$$M(x,t) = \underbrace{2B\int_0^{z_Y} E\varepsilon z dz}_{\textbf{elastic zone}} + \underbrace{2B\int_{z_Y}^{\frac{H}{2}} a\varepsilon^n \left(\frac{\dot{\varepsilon}}{\dot{\varepsilon}_0}\right)^m z dz}_{\textbf{rate dependent elasto plastic zone}} \tag{7}$$

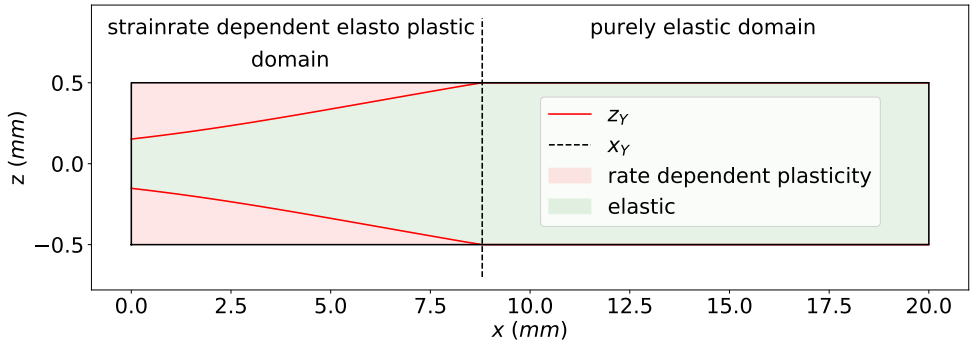

Figure 4: Expected domains in the cantilever beam

So far, $z_Y(x,t)$, $\varepsilon(x,z,t)$ and $\dot{\varepsilon}(x,z,t)$ are unknown. A simplification is obtained by Bernoulli Euler hypothesis [10] and [11], assuming that cross-sections remain plane and normal to the beam axis. Thus, the strain is linearly distributed over the entire cross-section, and can be expressed as

$$\varepsilon\left(x,z,t\right) = -w\left(x,t\right)'' z, \qquad \dot{\varepsilon}\left(x,z,t\right) = -\dot{w}\left(x,t\right)'' z. \tag{8}$$

By substituting Eq. (8) into Eq. (5), and considering that $w = w(x,t)$, $\dot{w} = \dot{w}(x,t)$, an additional condition for the yield height z_Y is obtained as

$$z_Y = \left[-\frac{a}{w''}\left(\frac{-\dot{w}''}{\dot{\varepsilon}_0 E}\right)^{\frac{1}{1-n}}\right]^{\frac{1-n}{1-m-n}}. \tag{9}$$

Balancing the moment caused by the external force, Eq. (3), with the moment caused by the internal stresses , Eq. (7), and inserting (8), and considering that $z_Y = z_Y(x,t)$ we obtain

$$-P\left(t\right)\left(L-x\right) = 2B\left[\int_0^{z_Y} -w''zEzdz + \int_{z_Y}^{\frac{H}{2}} a\left(-w''z\right)^n\left(\frac{-\dot{w}''z}{\dot{\varepsilon}_0}\right)^m zdz\right] \tag{10}$$

Evaluating the integral yields

$$-P\left(t\right)\left(L-x\right) + \frac{2}{3}Bw''Ez_Y^3 = \frac{aB\left(-w''\right)^n\left(H^{2+m+n} - 2^{2+m+n}z_Y^{2+m+n}\right)}{2^{1+m+n}\left(2+m+n\right)}\left(\frac{-\dot{w}''}{\dot{\varepsilon}_0}\right)^m. \tag{11}$$

Inserting Eq. (9) yields a non-linear differential equation for the curvature of the cantilever, which can be solved numerically as shown in the following sections.

2.2 Numerical solution strategy

In rate-dependent plasticity the time dependency of the applied load is essential. In the following, we consider $P(t)$ as a ramp with amplitude $\hat{P}$ and loading time T,

$$P\left(t\right) = \hat{P}\frac{t}{T}, \tag{12}$$

For computing the solution for the curvature we must consider two zones as schematically shown in Figure 4: For $x \geq x_Y$, the well-known elastic relation , Eq. (13), is valid:

$$w\left(x,t\right)'' = \frac{12P\left(L-x\right)}{BH^3E} \tag{13}$$

In the plastic zone, $x < x_Y$, the curvature is given by a nonlinear differential equation following from Eqs. (9) and (11). Only a numerical solution is possible. For this purpose, the time-related change of the curvature is approximated by the difference quotient.

$$\dot{w}\left(x,t\right)'' \approx \frac{\Delta w\left(x,t\right)''}{\Delta t} \tag{14}$$

In order to estimate the curvature correctly, the load must be applied incrementally. In each step, it must be checked whether elastic or plastic deformation occurs at the point under consideration. Since the time function of the load is known, this can be done by computing the yield time t_Y, i.e. the time at which first plastification occurs.

Solving w'' from Eq. (9) and substituting into Eq. (11) results in an equation depending on z_Y. Plasticity occurs in the cross-section as soon as the yield height is $z_Y = \frac{H}{2}$. Inserting furthermore Eq. (12) gives

$$t_Y = \frac{BH^2ET}{6P\left(L-x\right)}\left(\frac{a\left(\frac{-\dot{w}''}{\dot{\varepsilon}_0}\frac{H}{2}\right)^m}{E}\right)^{\frac{1}{1-n}}. \tag{15}$$

The complete numerical procedure can be summarized as follows:

1. Iterative force application
2. Check for plasticity using Eq. (15)
   (a) $t \leq t_Y$: If not, calculation of curvature by means of Eq. (13)
   (b) $t > t_Y$: calculation of curvature by means of the differential equation following from Eqs. (9) and (11)
3. Check for correct choice (elastic/plastic)
4. Increase load

Once the curvature is determined, the bending angle can be calculated by numerical integration. With a further numerical integration, also the vertical deflection can be determined. For this purpose, a Python code has been written using the toolbox Scipy. The results are presented in the following section.

3 Numerical results

In this section the curvature, bending angle, vertical deflection, plastic zones and distribuation of the strain rate are analyzed. To find out a reasonable range for the load to be analysed, the force level causing first yield under quasi-static condition is determined. This force $P_{Y,qs}$ follows by substituting $P = P_{Y,qs}$, $t_Y = T$, $x = 0$ and $\frac{\varepsilon(z=H/2)}{\dot{\varepsilon}_0} = 1 = \frac{-\dot{w}''}{\dot{\varepsilon}_0}\frac{H}{2}$ into Eq. (15). The solution is

$$P_{Y,qs} = \frac{BH^2Y\left(\frac{a}{E}\right)^{\frac{1}{1-n}}}{6L}. \tag{16}$$

Furthermore we introduce the non-dimensional force λ as the relation of applied force and the quasi-static yield force.

$$\lambda = \frac{P}{P_{Y,qs}} \tag{17}$$

The process parameters have been chosen according to Table 1, and the material parameters according to Table 2.

Table 1: process parameters

process parameter	Value
length L	20 mm
height H	1mm
width B	1mm
total time T	0.3s
reference strain rate $\dot{\varepsilon}_0$	$0.001\frac{1}{s}$

Table 2: material parameters

material parameter	Value
Young's modulus E	$210\,000\frac{N}{mm^2}$
scaling factor a	$600\frac{N}{mm^2}$
hardening exponent n	0.2
strain rate sensitivity m	0.02

3.1 Beam theory results for $\lambda = 1.75$

In this first analysis the solutions for curvature, bending angle and the deflection of the cantilever for different material behavior are discussed. The following cases are analyzed:

- Purely elastic case, Eg. (13)
- Elasto-plastic case, solution from [2] (without strain rate sensitivity)
- Rate dependent plasticity

Figure 5 shows the curvature, angle and displacement of the fully loaded beam for the different cases

In the purely elastic case, the curvature is linear along the axis. In the elasto-plastic case, and also in the rate-dependent plastic case, the curvature is nonlinear in the elasto-plastic zone, and linear in the elastic region ($x > x_Y$). In all cases, the highest curvature

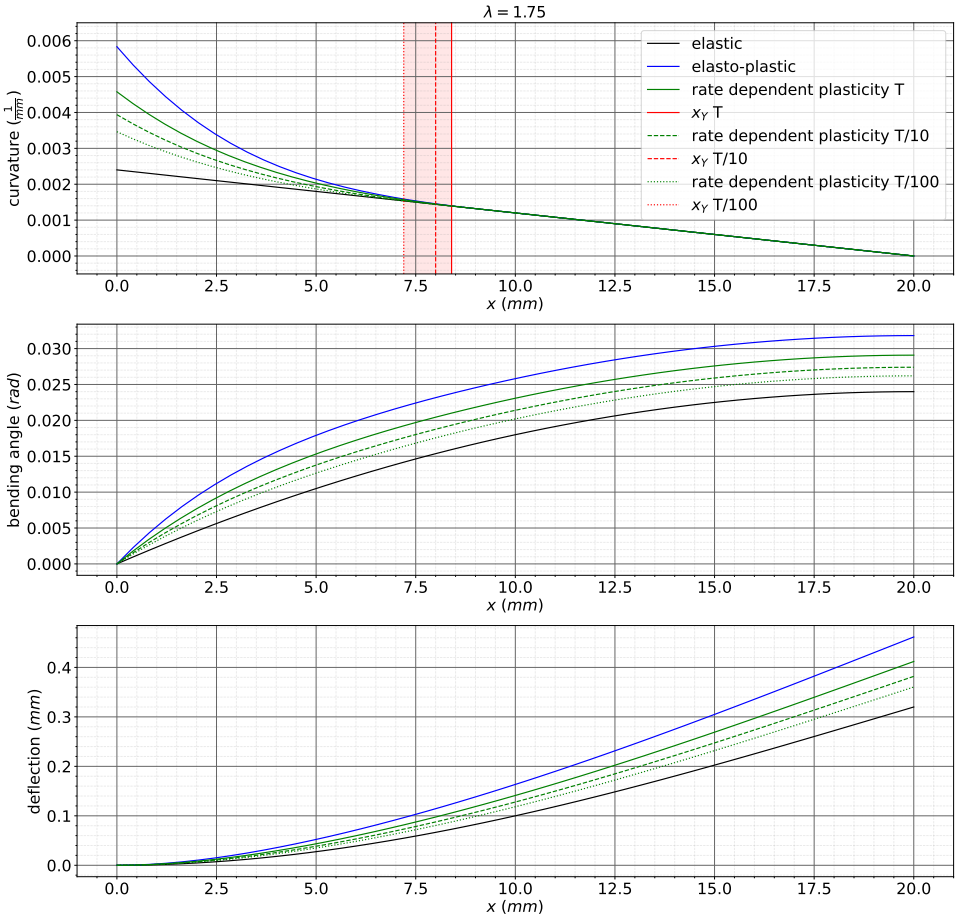

Figure 5: Curvature, angle and deflection of different material behavior

occurs at the clamped end ($x = 0$). With a purely elastic material behavior, the curvature is lowest. For the rate-dependent case, three values for the loading time T are compared. The lower T, the higher are the strain rates in the beam. This leads to an additional hardening of the beam. The bending angle and the vertical displacement show a very similar behavior. These results are maximum at the free end of the cantilever in all cases.

With the results in Figure 5 the boundaries of the elastic and the plastic domain can be evaluated. The results are shown in Figure 6. With increasing strain rate (decreasing loading time T) the elasto-plastic zone decreases. With the difference quotient it is also possible to calculate the distribution of stress, strain and the strain rate for the whole domain. Results are shown in the next chapter as contour-plots, compared to Finite Element results.

3.2 Verification by Finite Elements

For the following analyses, the parameters of tables 1 and 2 are used. To verify the results of beam theory, a Finite Element (FE) model of the cantilever beam has been implemented in Abaqus, using 3D continuum elements and considering geometric non-

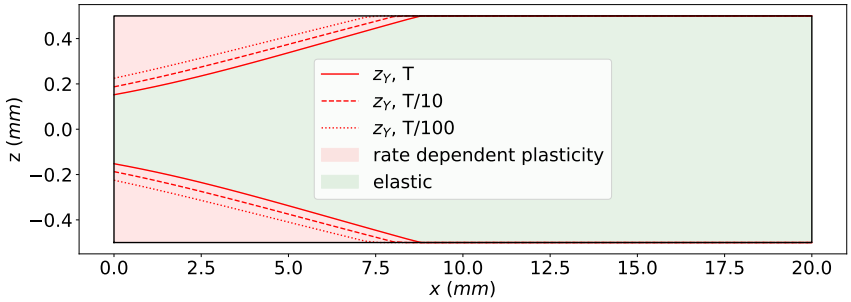

Figure 6: Elastic and rated dependent elasto plastic domain

linearity. Since inertial forces can be neglected in the considered process, a quasi-static analysis is sufficient. In Abaqus, the material behaviour including strain rate sensitivity can be defined in form of tables, [12].

Figure 7 shows the calculated deflection from beam theory and the FE model. If the deflection of the purely elastic beam is considered, a high agreement between theory and FE calculation is obtained. With the elasto-plastic material behavior, according to [2], there is still a high agreement with the FE simulation results. Comparing the results for the rate-dependent cases, there are also only minor deviations. With increasing strain rate, the deviations increase slightly.

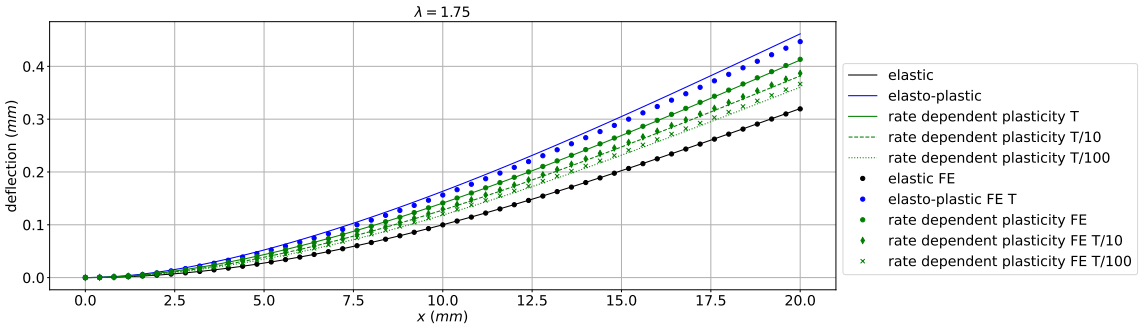

Figure 7: Comparison of the deflection theory and FEM

In the next step, contour plots of strain, strain rate and stress are shown in Figures 8 to 13, comparing the results of the FE model and the theoretical analysis. For the strain field, Figures 8 and 9, a high agreement is observed. Only near the boundary there are discrepancies. The reasons are deviations from the uniaxial state of stress due to the clamped boundary which are not considered in Bernoulli Euler beam theory. This is also a reason for the deviations in the deflection between FE and theory. The strain rate is the time derivative of the strain. Accordingly, Figures 10 and 11 show also a good agreement between theory and simulation for the strain rate. Finally, there is also a high level of agreement for the stress as shown in Figures 12 and 13.

Finally, a parameter study has been performed varying B, T and λ to estimate the

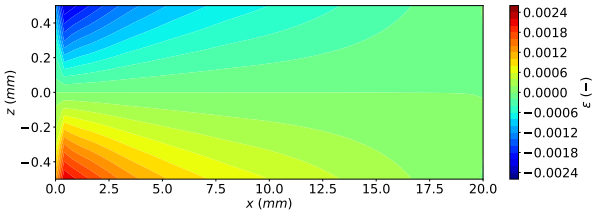

Figure 8: Calculated strain FEM

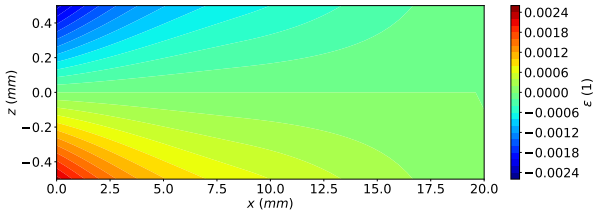

Figure 9: Calculated strain theory

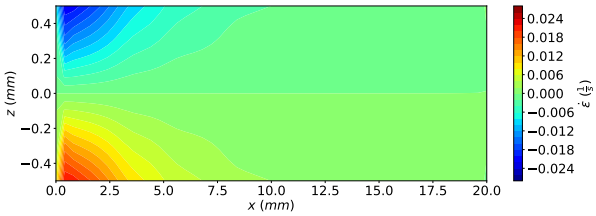

Figure 10: Calculated strain-rate FEM

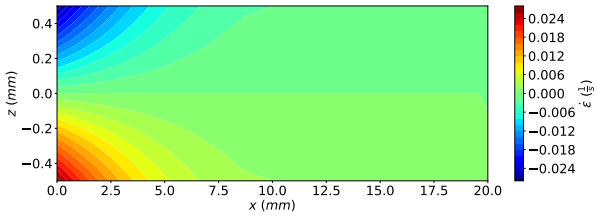

Figure 11: Calculated strain-rate theory

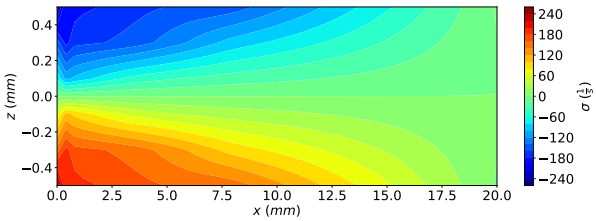

Figure 12: Calculated stress FEM

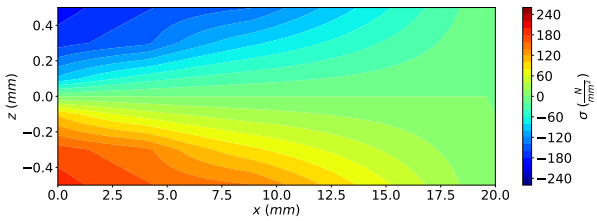

Figure 13: Calculated stress theory

valid range of the theoretical considerations. The relative deviation between FEM and Theory can be expressed as follows

$$\Psi = \frac{w_{\text{Theory}}\left(L,T\right) - w_{\text{FEM}}\left(L,T\right)}{w_{\text{FEM}}\left(L,T\right)}. \tag{18}$$

Table 3 shows the results of the parameter study. In general, there is a good agreement. For shorter beams the agreement between FEM and theory is reduced, as it is the case if the width is increased. This behaviour was expected because the conditions for a Bernoulli-Euler beam are less accurate in this cases. All in all the coincidence of beam theory and Finite Element method is very good.

Table 3: Results parameter study (elasto-visco-plastic material behavior)

L $[mm]$	H $[mm]$	B $[mm]$	T $[s]$	λ [1]	Ψ [%]	L $[mm]$	H $[mm]$	B $[mm]$	T $[s]$	λ [1]	Ψ [%]
20	1	1	0.3	1.25	0.13	10	1	1	0.3	1.75	0.93
20	1	1	0.03	1.25	0.17	10	1	1	0.03	1.75	-0.06
20	1	1	0.003	1.25	0.04	10	1	1	0.003	1.75	-0.81
20	1	1	0.3	1.75	-0.44	5	1	1	0.3	1.75	2.50
20	1	1	0.03	1.75	-1.37	5	1	1	0.03	1.75	0.64
20	1	1	0.003	1.75	-1.80	5	1	1	0.003	1.75	-0.76
20	1	1	0.3	2.5	3.96	20	1	3	0.03	1.75	2.42
20	1	1	0.03	2.5	1.61	20	1	5	0.03	1.75	5.07
20	1	1	0.003	2.5	-0.74						

4 CONCLUSIONS

In this work, a rate-dependent material behavior in the framework of Bernoulli-Euler beam theory has been investigated for the example of a cantilever with a transverse tip force. The theoretical analyses show a very high agreement with FE solutions, especially for slender beams for which Bernoulli-Euler assumption holds.

As expected, and also observed on an industrial panel bender, the results show that an increasing strain rate causes an increase of the beam stiffness, having influence on the curvature of the beam. With the outcome of this paper, i.e the implemented simulation models, the influence of highly rate-sensitive materials on the geometric dimensions of the final product and the process forces can be computed.

Future possible extensions of the theory work concern a refinement of the proposed beam model for a better coincidence with the industrial panel bending process, e.g. extension of the theory for plates, and higher deformations. Furthermore, it is also planned to extend the models of the digital twin in [1] to consider strain rate sensitivity in the adaptive bending strategy.

ACKNOWLEDGEMENT

This work has been supported by the COMET-K2 “Center for Symbiotic Mechatronics” of the Linz Center of Mechatronics (LCM) funded by the Austrian federal government and the federal state of Upper Austria.

REFERENCES

[1] C. Zehetner, C. Reisinger, W. Kunze, F. Hammelmüller, R. Eder, H. Holl and H. Irschik *High-quality sheet metall production using a model based adaptive approach.* Procedia Computer Science, 2021, 180, 249-258.

[2] C. Zehetner, F. Hammelmüller, H.Irschik and W. Kunze *Similarity methods in elasto-plastic beam bendung.* Complas XIII: proceedings of the XIII International Conference

on Computational Plasticity: fundamentals and applications, 2015, 906-915.

[3] H. Hollomon *Tensile deformation*. Aime Trans vol. 12, no. (4). 1945.

[4] P. Ludwik *Elemente der technologischen Mechanik*. Springer Verlag Berlin, 1909.

[5] E. Voce *The relationship between stress and strain for homogeneous deformation*. J. Int. Metals , 1948, 537-562.

[6] D.V. Wislon *Strain rate sensitivity and effects of strain rate sensitivity on sheet metalforming*. Met. Technol., 1980.

[7] G.R.Johnson and W.H.Cook *A constitutive model and data for metals subjected to large strains, high strain rates and high temperatures*.Proc. of the 7th Int. Symposium on Ballistics, 1983, The Hague, 541-547.

[8] G.R. Cowper, P.S. Symonds *Strain hardening and strain rate effects in the impact loading of cantilever beams.*. Brown University Appl. Math. Report, 28 1958, 1-46.

[9] P. Larour *Strain rate sensitivity of automotive sheet steels: influence of plastic strain, strain rate, temperature, microstructure, bake hardening and pre strain*. Thesis (Phd), Rheinisch-Westfälische Technische Hochschule Aachen, 2010.

[10] F. Ziegler *Mechanics of Solids and Fluids*. Springer Verlag, 1995.

[11] D. Gross, W.Hauger, J. Schröder, W.A. Wall and J. Bonet *Engineering Mechanics 2*. Springer Verlag, 2018.

[12] D. S. Simulia *Abaqus Dokumentation*. 2019.